2.3

USING IMPROVED BACKGROUND ERROR COVARIANCES FROM AN ENSEMBLE KALMAN FILTER FOR TARGETED OBSERVATIONS

Thomas M. Hamill

NOAA-CIRES Climate Diagnostics Center, Boulder, Colorado

Chris Snyder

National Center for Atmospheric Research, Boulder, Colorado*

1. INTRODUCTION

Assume that in addition to a routine network of observations, additional observations could be collected sporadically for a moderate cost. These observations, which might come from dropsondes, pilotless drones, or driftsondes, would be taken at a location(s) chosen to maximize the expected improvement in some aspect of the ensuing analysis or the subsequent forecasts. This general problem is known as *targeting*, or *adaptive observations*.

We consider here the targeting problem on a somewhat theoretical level. Choosing optimal observation locations requires that we accurately predict the expected reduction in uncertainty of the analysis or subsequent forecast due to assimilating an observation. That influence is determined not only by the form and accuracy of the observation and how errors grow during the forecast (if we are interested in forecasts); it also depends on the prior or "background" uncertainty, which is a function of the prior forecasts and observations. Berliner et al. (1999) provide the analytical tools for understanding how analysis and forecast uncertainty are related to observation and background uncertainty. This framework differs from many of the existing approaches that do not consider the effects of background uncertainty, such as the singular vector or sensitivity techniques. As a consequence, when using these techniques, the same target location is selected regardless of how large or small the background error is in a given location, and regardless of how accurate or inaccurate the observation (Baker and Daley 1999).

Our primary intent in this preprint is to demonstrate a relatively simple, objective, and computationally efficient algorithm for target selection based on and consistent with Berliner et al. (1999). To wit, we shall use an ensemble of forecasts coupled to three different data assimilation schemes, including two variants of the ensemble Kalman filter ("EnKF;" Evensen 1994; Houtekamer and Mitchell 1998). We demonstrate that a target selection algorithm with an accurate model of background error covariances provided by a large ensemble is able to identify target locations where analysis improvement is likely to be the largest. Its straightforward and computationally efficient design permits it to estimate the magnitude of the variance reduction at each of a multitude of possible target locations; the targeting algorithm then selects the location where this variance is reduced by a maximum expected amount.

We will focus on testing the algorithm to reduce analysis, not forecast errors. Details on a similar approach for reducing forecast errors as well as much more detail on this scheme is available in a manuscript, available from the author (Hamill and Snyder 2001, "HS01").

2. DESIGN OF THE EXPERIMENT

a. Model and Observations

The rest of the paper will use a quasigeostrophic (QG) channel model as vehicle for testing algorithms for targeting. The QG model was used in Hamill et al. (2000) and HS01. The forecast model is assumed perfect. A long reference integration of the QG model provides the true state; the assimilation and forecast experiments then use that same model together with imperfect observations of the true state. Errors will be measured in a total energy norm, defined in HS01.

A single fixed observational network is tested here (Fig. 1), with a data void in the western third of the domain. All observations are presumed to be rawinsonde soundings, with u- and v-wind components and θ observed at each of the 8 model levels. Observation errors are assumed to be normally distributed, uncorrelated between vertical levels, and uncorrelated in time.

b. Data assimilation schemes.

* The National Center for Atmospheric Research is sponsored by the National Science Foundation

Corresponding author address: Dr. Thomas M. Hamill, NOAA-CIRES CDC, R/CDC 1, 325 Broadway, Boulder, CO USA 80303 ; e-mail: hamill@cdc.noaa.gov

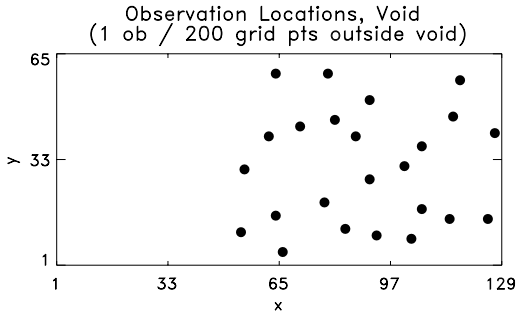

Figure 1. Location of fixed raobs for network with data void.

We will test the targeting scheme using three different ensembles as input. One, an "inflated" ensemble, uses an ensemble Kalman filter with inflation of covariances to address the problem of filter divergence (see discussion of filter divergence and possible remedies in Hamill et al. 2001). Another "hybrid" ensemble uses a blend of background error covariances estimated from the ensemble and from a stationary, 3D-Var model. The final, "perturbed observation" ensemble, uses strictly stationary "3D-Var" background error covariances. Details of the data assimilation are provided in HS01.

3. STRATEGY FOR CHOOSING TARGET LOCATIONS TO MINIMIZE ANALYSIS ERROR VARIANCE

a. Background

Consider the analysis process within the standard Kalman filter / estimation theory framework under perfect model assumptions. Recall that the m-dimensional analyzed state vector $\mathbf{x}^a$ in an extended Kalman filter is found by updating the background state $\mathbf{x}^b$ to a new set of new observations $\mathbf{y}^o$, weighted by the Kalman gain matrix $\mathbf{K}$:

$$\mathbf{x}^a = \mathbf{x}^b + \mathbf{K}\left(\mathbf{y}^o - \mathbf{H}\mathbf{x}^b\right). \tag{1}$$

Observations have unbiased and normally distributed errors, defined by

$$\mathbf{y}^o = \mathbf{H}\mathbf{x}^t + \epsilon, \quad \epsilon \sim N(0, \mathbf{R}) \tag{2}$$

and $\mathbf{H}$ is an operator converting the model state to the observation locations and types. $\mathbf{K}$ is defined by

$$\mathbf{K} = \hat{\mathbf{P}}^b\mathbf{H}^T\left(\mathbf{H}\hat{\mathbf{P}}^b\mathbf{H}^T + \mathbf{R}\right)^{-1}. \tag{3}$$

$\hat{\mathbf{P}}^b$ is an estimate of the true background error covariance matrix $\mathbf{P}^b$. When coupled together with a forecast model and a method for propagating background error covariances, equations (1)-(3) provide a general analysis system. Assuming that the observation and background errors are uncorrelated, i.e., $\left\langle \epsilon\left(\mathbf{x}^b - \mathbf{x}^t\right)^T \right\rangle = 0.$ and substituting the definition of $\mathbf{K}$ from (3), the expected analysis error variance is

$$\mathbf{P}^a = \mathbf{P}^b - \mathbf{K}\mathbf{H}\mathbf{P}^b - \left[\mathbf{K}\mathbf{H}\mathbf{P}^b\right]^T + \mathbf{K}\left(\mathbf{H}\mathbf{P}^b\mathbf{H}^T + \mathbf{R}\right)\mathbf{K}^T \tag{4}$$

If the background error covariance estimate is perfect, $\hat{\mathbf{P}}^b = \mathbf{P}^b$, then (4) simplifies to the more familiar

$$\mathbf{P}^a = \left(\mathbf{I} - \mathbf{K}\mathbf{H}\right)\hat{\mathbf{P}}^b = \hat{\mathbf{P}}^b - \hat{\mathbf{P}}^b\mathbf{H}^T\left(\mathbf{H}\hat{\mathbf{P}}^b\mathbf{H}^T + \mathbf{R}\right)^{-1}\mathbf{H}\hat{\mathbf{P}}^b, \tag{5}$$

where $\mathbf{I}$ is the $m \times m$ identity matrix. (4) and (5) thus provide us with a framework for estimating analysis error variances for a given $\mathbf{H}$ in the case of imperfect and perfect background error statistics, respectively.

Suppose we want to find the observation location (i.e., the operator $\mathbf{H}$) that minimizes the expected analysis error variance. Assume hereafter that a relatively large ensemble is available and that this ensemble is constructed in a manner so that $\hat{\mathbf{P}}^b$ can be estimated reasonably from the ensemble, $\hat{\mathbf{P}}^b \simeq \mathbf{P}^b$. (5) then can be used to evaluate the expected error variance reduction from assimilating that observation prior to assimilating the actual observation. The second term in (5) denotes the expected reduction in error covariance due to assimilating the new observations. This then suggests an algorithm for targeting. Loop through all the potential observation locations that could potentially be targeted. Build the operator $\mathbf{H}$ for a location, and evaluate $Tr\left[\hat{\mathbf{P}}^b\mathbf{H}^T\left(\mathbf{H}\hat{\mathbf{P}}^b\mathbf{H}^T + \mathbf{R}\right)^{-1}\mathbf{H}\hat{\mathbf{P}}^b\right]$ at this location (that is, the sum of the variance reduction). Proceed to the next location. After the trace is determined at all locations, target the observation location (or more specifically, the $\mathbf{H}$) where the trace is largest.

Two points are worth emphasizing. First, suppose we have a very imperfect model of background error covariances, perhaps as are used in 3D-Var. Then (4) should be used instead of (5), and estimation of the variance reduction using (4) still requires knowledge of the true statistics, as can be seen by the terms involving $\mathbf{P}^b$ in (4). Second, it is statistically valid in the extended Kalman filter (slightly less so in the EnKF) to assimilate observations sequentially if background error covariances are updated (Anderson and Moore 1979). The analysis error covariance estimate after assimilation of the first observation thus is used as background error covariance for the assimilation of the second observation, and so on.

b. Making the targeting algorithm computationally efficient

For brevity, we will not provide details here. The reader is referred to a full description of the algorithm in HS01. The major simplification is to transform

the problem to work in the subspace spanned by the eigenvectors of the background error covariance matrix estimated from the ensemble.

4. PERFORMANCE OF THE ENSEMBLE DATA ASSIMILATION METHODS.

Before demonstrating the target selection method, we briefly note the general performance of the three data assimilation methods using the observations at the fixed network of rawinsondes in Fig. 1. For each of the three assimilation methods, a 90-day cycle of short-range forecasts and analyses were generated here, with an updated analysis generated every 12 hours.

The analysis errors for the three ensembles are quite different; the ensemble mean error for the inflated, hybrid, and perturbed observation ensembles averaged over the 90-day period are 1.07, 1.34, and 8.15 ms^{-1}, highlighting the dramatically improved accuracy achieved by using a flow-dependent model of covariances in the EnKF (though the relative improvement may be misleading of the results in real-world weather prediction, since these experiments are conducted with a relatively simple model in a perfect-model framework).

5. TARGETED OBSERVATION RESULTS.

a. Targeting with full algorithm

We now test the scheme that selects the target location which will maximize the expected reduction in analysis error variance (eq. 5). The targeting results shown here are primarily based on a subset of 20 of the times in this series, starting ten days into the analysis cycle and every 4 days thereafter. The analyses produced by the assimilation of the fixed network of raobs are used as the background states for the targeting tests performed here. This is a justifiable assumption to make if the observations are assimilated sequentially.

To evaluate the errors of the targeting algorithm, we note that standard statistical result that for a random sample of the vector $\mathbf{x}^a$ with sample mean $\overline{\mathbf{x}}^a$ and true state $\mathbf{x}^t$

$$\left\langle (\mathbf{x}^a - \mathbf{x}^t)(\mathbf{x}^a - \mathbf{x}^t)^T \right\rangle = \left\langle (\overline{\mathbf{x}}^a - \mathbf{x}^t)(\overline{\mathbf{x}}^a - \mathbf{x}^t)^T \right\rangle + \left\langle (\mathbf{x}^a - \overline{\mathbf{x}}^a)(\mathbf{x}^a - \overline{\mathbf{x}}^a)^T \right\rangle \quad (6)$$

The analysis error variance in (6) is composed of two terms, the *mean squared error* and the *sample variance*, respectively. It can be shown that these if the true state and the analyzed states can be considered random samples from the same probability distribution, then the two terms should be equal in expected value.

Ensembles from each of the three data assimilation systems were used for target selection under the assumption that the ensemble could provide a perfect model of the covariances, i.e., (5) could be used instead of (4) to assess the impact if an EnKF were used for the data assimilation. The computationally efficient targeting algorithm was used to compute $Tr(\mathbf{KH\hat{P}}^b)$ for each horizontal grid point in the domain for each of the twenty case days. Figure 2 provides maps of the patterns of expected fractional reduction in analysis error for one of the case days using the inflated ensemble. Note that a synthetic observation was actually assimilated, with concomitant dramatic reductions in analysis variance, as illustrated in panel (c) of Fig. 2. To statistically assess the improvement, for each of the 20 case days, the optimal target location was determined for the inflated,

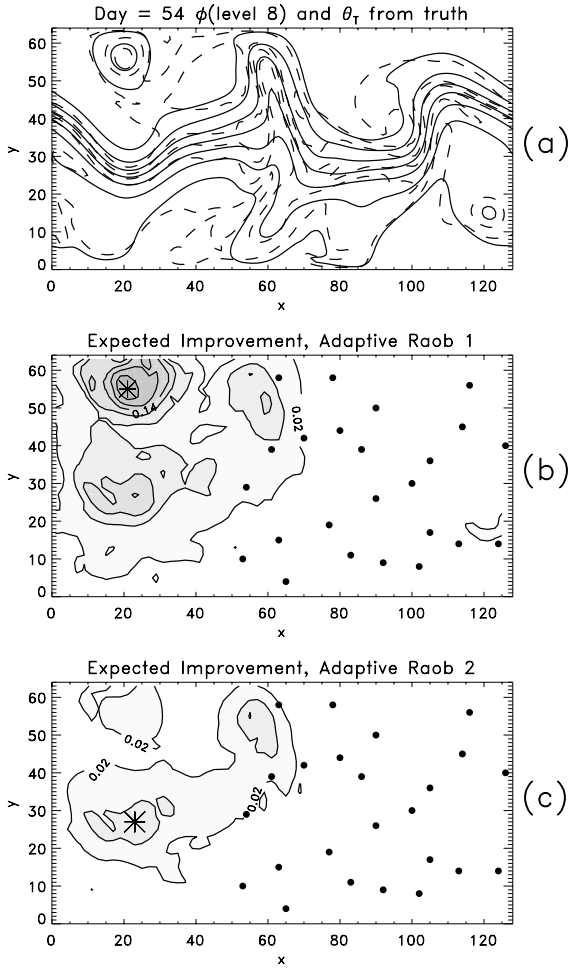

Figure 2. Expected fractional reduction in analysis sample variance from application of targeting algorithm on Day 14 of the 90-day integration of the inflated ensemble assimilation scheme. (a) True geopotential height (solid) at model level 8 and θ_T (potential temperature on top lid; dashed). (b) Expected fractional reduction in analysis sample variance mapped for each potential observation location in the domain. Dots indicate locations of fixed network of observations previously assimilated. Star indicates location of maximum expected reduction (the target location). Contours at 2 percent and every 4 percent thereafter. (c) As in (b), but the improvement after the first targeted observation has been assimilated.

hybrid, and perturbed observation ensemble using (5). Because the accuracy of the subsequent analysis may depend upon the actual errors of the observation, for each case day we generated 5 independent realizations of the control observations by adding errors to the true state, with the errors consistent with **R**. Each observation was then separately assimilated using the same set of background forecasts.

Figs. 3 (a)-(c) plots expected fractional reduction in analysis error variance vs. fractional reduction of ensemble mean error variance for the inflated, hybrid, and perturbed observation ensembles, respectively. The expected reduction in variance and the actual reduction in ensemble mean error are roughly consistent for the inflated and hybrid ensembles; generally, larger expected reductions in the ensemble mean error are associated with larger expected reductions in analysis variance. However, the actual reduction for the perturbed observation ensemble is much less than predicted. This is a consequence of the actual data assimilation being performed with 3D-Var while the targeting algorithm assumes that the assimilation is performed with an EnKF. Now, suppose that the ensemble really does provide an accurate model of $\mathbf{P}^b$, but the much less accurate 3D-Var statistics are to be used for the data assimilation. Then we can evaluate the improvement from a targeted observation based on equation (4) instead of (5); here, we compute the trace of (5) assuming $\hat{\mathbf{P}}^b$ is the stationary, 3D-Var covariance model and $\mathbf{P}^b$ is the covariance estimate from the perturbed observation ensemble. Fig. 3 (d) shows the reduction under these assumptions.

b. Improvement from targeted vs. fixed observations.

We now attempt to provide an estimate of the benefit of assimilating a supplemental targeted observation relative to assimilating a fixed observation in the middle of the void. We test this in two manners; first, we compare the analysis error reduction when either a fixed or targeted observation is intermittently assimilated. Next we consider the case if a targeted or new fixed observation is available at every data assimilation cycle.

Using the inflated ensemble and the set of 20 times used previously, we applied the targeting algorithm. The fractional reduction in the ensemble mean analysis error (the first term in (6)) was computed and then compared it to the fractional reduction that would be achieved with a fixed supplemental raob profile at the grid point (30,33), in the middle of the void. A scatterplot of the reduction is shown in Fig. 4. There is a dramatic improvement from using the targeted observation relative to the fixed observation. The mean improvement is over 20 percent for the targeted observation, approximately 4.5 percent for the fixed. The targeted observation improved the analysis in 19 of 20 cases vs. only 15 of 20 for the fixed.

We also performed an experiment where one observation profile in the middle of the data-rich region was removed (the observation at x=80, y=45 in Fig. 1), and either a new fixed observation at (30,33) or a targeted

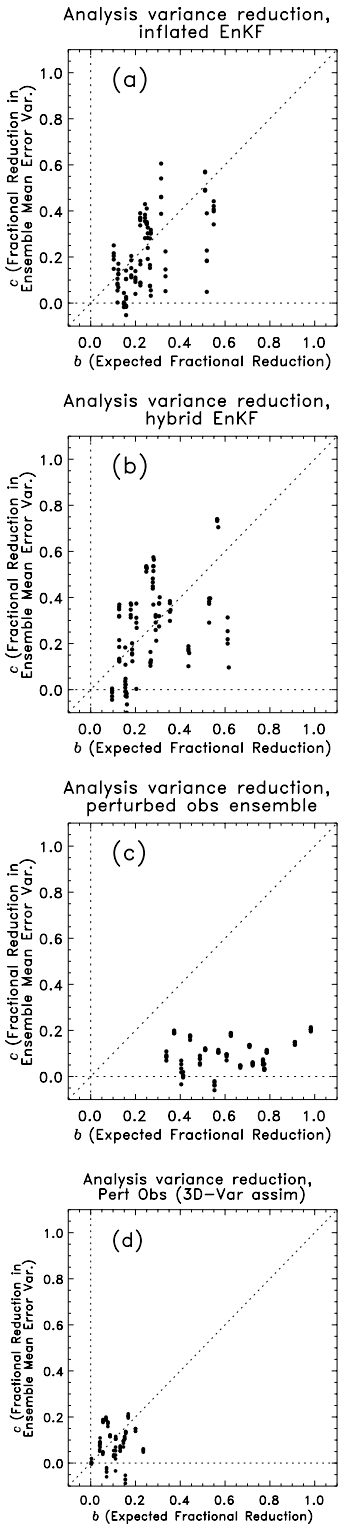

Figure 3. (a) Actual fractional reduction in ensemble mean variance c vs expected fractional reduction in analysis error variance b for optimal target locations from inflated ensemble. Five independent control observations tested for each of the 20 case days. (b) As in (a), but for hybrid ensemble, and (c) As in (a), but for perturbed observation ensemble. (d) As in (c), but where eq. (4) is used instead of (5) to predict expected improvement.

observation was assimilated *during every cycle.* The relative improvement now is not nearly as dramatic (Fig. 5). There are substantial reductions in the ensemble mean analysis error from inserting a fixed observation in the middle of the void (compared to the ensemble mean error of 1.07 from standard network). With a targeted observation, there is further improvement, but not to the extent suggested from the experiments where a targeted observation was introduced intermittently. There may be a number of factors which limit the improvement with cycled targeted observations. First, relatively quickly, the targeted observations tamp down the background variance in the data void. The primary benefit of targeted observations occurs when the background errors are quite large; then the observation has a great impact. When a targeted observation is continually assimilated, it reduces the maximum background errors substantially, and errors are not likely to grow back to their original magnitude in the 12 h to the next assimilation cycle. Thus, in some sense a targeted observation can make subsequent targeted observations less neccessary. Another possibility is that features with high errors eventually flow near enough by the fixed observation in the middle of the void to be effectively corrected using the EnKF covariances.

6. CONCLUSIONS.

We demonstrate that use of an ensemble Kalman filter, which can improve the accuracy of analyses by providing an accurate, flow-dependent estimate of background error covariances, also may be used for adaptive observations. Improvements are estimated in a manner that is fully consistent with the optimal estimation theory underlying modern data assimilation.

REFERENCES

Anderson, B. D., and J. B. Moore, 1979: Optimal filtering. Prentice-Hall, Inc., 357 pp.

Baker, N. L, and R. Daley, 2000: Observation and background adjoint sensitivity in the adaptive observation-targeting problem. *Quart. J. Roy. Meteor. Soc.*, **126**, 1431-1454.

Berliner, L. M., Z.-Q. Lu, and C. Snyder, 1999: Statistical design for adaptive weather observations. *J. Atmos. Sci.*, **56**, 2536-2552.

Bishop, C. H., B. J. Etherton, and S. J. Majumdar, 2001: Adaptive sampling with the ensemble transform Kalman filter. Part 1: Theoretical aspects. *Mon. Wea. Rev.*, **129**, 420-436.

Evensen, G., 1994: Sequential data assimilation with a nonlinear quasigeostrophic model using Monte Carlo methods to forecast error statistics. *J. Geophys. Res.*, **99 (C5)**, 10143-10162.

Hamill, T. M., C. Snyder, and R. E. Morss, 2000: A comparison of probabilistic forecasts from bred, singular vector, and perturbed observation ensembles. *Mon. Wea. Rev.*, **128**, 1835-1851.

——— , and ——— , 2001. Targeted observations using improved background error covariances from an ensemble Kalman filter. *Mon. Wea. Rev.*, submitted. Available at www.cdc.noaa.gov/∼hamill

——— , J. S. Whitaker, and C. Snyder, 2001: Distance-dependent filtering of background error covariances in an ensemble Kalman filter. *Mon. Wea. Rev.*, accepted. Available at www.cdc.noaa.gov/∼hamill

Houtekamer, P. L., and H. L. Mitchell, 1998: Data assimilation using an ensemble Kalman filter technique. *Mon. Wea. Rev.*, **126**, 796-811.

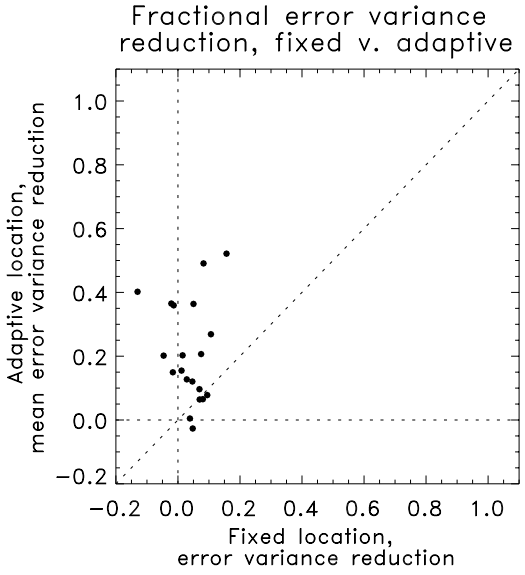

Figure 4. Improvement in ensemble mean analysis error when assimilating targeted vs fixed observations on each of 20 case days.

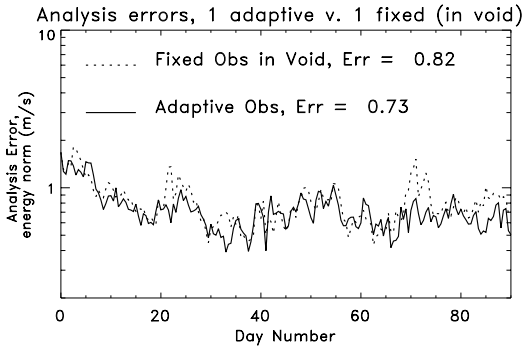

Figure 5. Time series of ensemble mean analysis errors when replacing observation profile at (80,45) in the data assimilation cycle with either a fixed profile at (30,33) or a targeted observation.